Spanish Journal of Agricultural Research
19 (2), e0206, 13 pages (2021)
eISSN: 2171-9292
https://doi.org/10.5424/sjar/2021192-15463
Instituto Nacional de Investigación y Tecnología Agraria y Alimentaria (INIA)

RESEARCH ARTICLE

OPEN ACCESS

Comparative performance analysis of innovative separation chamber configurations: Numerical and experimental investigations

Mansour Zobeiri, Vahid Rostampour, Adel Rezvanivand-Fanaei and Ali M. Nikbakht

Urmia University, Dept. of Mechanical and Biosystems Engineering, Urmia, Iran

Abstract

Aim of study: Novel configurations of separation chamber are proposed to resolve the critical issue of separation in agro-industrial equipment.

Area of study: Dept. of Mechanical and Biosystems Engineering, Urmia, Iran

Material and methods: Precise and instrumented experimentation has been conducted to calibrate the computational fluid dynamics (CFD) methodology in the modeling and simulating chickpea pod separation. Mechanisms were selected based on optimizing separation efficiency, relative purification and required airflow as a criterion for energy consumption.

Main results: Applying a guiding blade and suction fans may potentially increase the separation efficiency while reducing the relative purification and required airflow. The highest separation efficiency (95%), the lowest required airflow (545 m^3/h) and the lowest pressure drop (16.3 Pa), were obtained by such configuration. Furthermore, the highest relative purification of 90% was achieved when the mechanism was free of blade and fans.

Research highlights: To integrate the advantages of the above-mentioned configurations, a series-type assembling them is proposed to preserve the separation efficiency and relative purification at the highest level, meanwhile reducing the required airflow. Also, 15% enhancement in the separation efficiency and 302.8 m^3/h reductions in the airflow were found as a crucial finding. The high correlation of experimental and theoretical CFD results is the key point to motivate the researchers for extension of similar case projects.

Additional key words: CFD; HSPh; purification; separation chamber

Abbreviations used: CFD (Computational Fluid Dynamics); DRSM (Differential Reynolds Stress models); HSPh (High Speed Photography); LDA (Laser Doppler Anemometry); LES (Large Eddy Simulation)

Authors' contributions: Conceived and designed the studies: MZ, VR. Performed the lab tasks: MZ, VR and ARF. Analysed the data and wrote the draft manuscript: VR, ARF and AMN. CFD simulations: VR, ARF. All the authors reviewed and corrected the text.

Citation: Zobeiri, M; Rostampour, V; Rezvanivand-Fanaei, A; Nikbakht, AM (2021). Comparative performance analysis of innovative separation chamber configurations: Numerical and experimental investigations. Spanish Journal of Agricultural Research, Volume 19, Issue 2, e0206. https://doi.org/10.5424/sjar/2021192-15463

Supplementary material: (Figs. S1, S2 and S3) accompanies the paper on SJAR's website.

Received: 14 Jul 2019. **Accepted:** 19 May 2021.

Funding: The authors received no specific funding for this work.

Competing interests: The authors has declared that no competing interests exist.

Correspondence should be addressed to Vahid Rostampour: v.rostampour@urmia.ac.ir; rostampoor2011@gmail.com

Introduction

Separation, purification, and the ability to handle grains and powders are the prominent aspects of industrial processes (Burtally *et al.*, 2002). The application of separation chambers is the separation of harvested pods and seeds from carrier air in products-harvesting machines such as chickpea, lentil, bean, etc. The problem of harvesting such products is challenging and researches have been carried out in this field (Zhao *et al.*, 2011; Gharakhani *et al.*, 2017). A detailed study of the chambers was conducted, proving the fact that improvement of design variables can increase the collection performance (Golpira *et al.*, 2013). Nowadays, the separation efficiency of the chambers used in chickpea harvesting machines is about 80%. Accordingly, separation efficiency improvement can bring many benefits, including economic aspects along with adequate efficiency (Motlagh *et al.*, 2018). To design the most efficient and cost-effective separation chamber (maximum separation, minimum required airflow, and minimum pressure drop), a piece of detailed information about the effect of different chamber design variables on the flow path characteristics is needed. These variables can include suction condition and flow path deviation. Since the effect of design parameters has not been studied on the fluid flows and optimum performance of

the separation chambers, a comprehensive investigation is required. An experimental study may determine the status of particle movement, but in order to obtain some conclusive results, numerical simulation techniques along with experimental tests should be conducted. Numerical simulations can progress an inexpensive way for predicting the results as well as the geometric optimization process.

Accordingly, extensive studies have been conducted considering separation and purification in various fields. Many studies have been conducted to expand the application of hydrocyclones by optimizing the effective variables and conditions (Tian *et al.*, 2018). Furthermore, separation methods and instruments have been developed in which a set of geometrical ratios has been optimized in cyclones to achieve the least pressure drop (Elsayed Khairy & Lacor, 2010). Also, membrane techniques, including both liquid and non-liquid membranes, have been investigated (Chen *et al.*, 2018). Generally, gas-solid separation is applied in segregation chambers, air filters, bag filters, cyclone separators, impingement separators, electrostatic and high -tension precipitators (Miller, 2014). On the other hand, for separation of comparatively large particles, segregation chambers, inertial separators, and cyclones are the most suitable choices (Krupińska *et al.*, 2018).

However, segregation chambers are the oldest and simplest equipment for separating the particles from an air stream without implementing any excessive filters in which the segregating factor is the air stream. Noteworthy, increment of the cross-section area at the chamber entrance reduces the airspeed in X direction of the stream so the particles would be segregated (Panasiewicz *et al.*, 2012). The advantages of segregation chambers include convenient construction, no moving parts, low investment and maintenance cost, and low pressure drop. The most crucial factors that affect the performance of the segregation chambers include the dimensions of the chamber, the uniformity of input material feeding, the velocity and relative humidity of air stream (Emami *et al.*, 2007; Krupińska *et al.*, 2018).

On the other hand, granular segregation is presented in different processes for many industries, including chemical, pharmaceutical, mining, food, agriculture, and different natural phenomena (Wei *et al.*, 2017). In the segregation method, air velocity is decreased at a particular part of the path flow. Accordingly, the particles are segregated from the air flow due to imbalances between particle density and air pressure. Möbius *et al.* (2001) found that particle density has a significant effect on the separation process, and the density dependence is sensitive to the background air pressure.

Different aspects of the particle removal from the gas stream have been studied in the segregation chamber. Chen *et al.* (2017) stated that dimensions, shape, weight, density, and adhesiveness should be calculated in addition to the concentration of the segregated particles. Various studies have been conducted to complete the separation and purification performance of the segregation chambers (Molerus & Glückler, 1996). Collection efficiency and pressure drop of two single cyclones with central hopper and side wall beside twin cyclone were evaluated by Ha *et al.* (2011). The separation efficiency was carried out using DMT (Deutche Montan Technologie) test.

Computational fluid dynamics (CFD) is a numerical technique that is widely used for the simulation of complex flows and has been included as an essential tool for the engineering design goals to predict the performance of newly proposed designs or processes before manufacturing (Rezvanivand Fanayi & Nikbakht, 2015; Devarrewaere *et al.*, 2016). A multiphase CFD model (mixed model) with sub-modules was used to simulate the performance of the hydrocyclones and predict velocity field extracted from the Large Eddy Simulation (LES) and Differential Reynolds Stress (DRSM) turbulence models and subsequently is compared with the Laser Doppler Anemometry (LDA) measurements (Narasimha *et al.*, 2012). Also, CFD was used to optimize a cyclone type spray chamber with a flow spoiler, designed to provide satisfactory efficiency (Schaldach *et al.*, 2003). Furthermore, CFD simulation was employed to investigate the effect of including the vertical baffle at the feed section of a separation tank for the improvement of solid segregation in potable water treatment (Goula *et al.*, 2008). Gebrehiwot *et al.* (2010) used the CFD technique to examine the flow configuration inside the combined cleaning chamber. Olatunde *et al.* (2017) used CFD to investigate the airflow distribution inside a rice bin storage system with different grain mass configurations. Moreover, Scotto di Perta *et al.* (2016) studied wind tunnel configurations effects with CFD simulation on the aerodynamic performances of the wind tunnels. A hybrid Euler–Lagrange approach was used for numerical simulation of a dense solid particle flow inside a cyclone separator. The simulations were performed for various inlet velocities of the gaseous phase and mass particle loadings. In addition, the influences of several sub-model variables on the results were studied (Kozołub *et al.*, 2017). Also, a novel computational framework entitled "System Coupling" was developed at ANSYS Inc. that simulates complex multi-physics coupled problems and prepares comprehensive validation and verification researches (Chimakurthi *et al.*, 2018). Characteristics of a percussive gas-solid separator as an experimental study and numerical simulation were studied and conducted, increasing both inlet velocity and negative pressure of the exhaust gas outlet improves separation efficiency (Wu *et al.*, 2018). Huang & Kuo (2017, 2018) simulated a rotating drum by CFD, and proposed the bed surface fitting (BSF) method to specify the suitable solid phase kinetic viscosities of granular flows. In the sugar beet processing of a sugar factory, a thermo-vapor-compressor simulation

was studied to reduce energy consumption in the crystallization section. In this study, dead steam was recovered by a thermo-compressor and reused in the processing units (Rezvanivand-Fanaei *et al.*, 2019). CFD also used as a numerical method to energy saving in a processing unit (Rezvanivand-Fanaei *et al.*, 2021). However, a comprehensive CFD simulation has not been performed to investigate the airflow distribution in agricultural separation chambers.

According to the comprehensive literature review, scientific literature lacks on investigating a proper separation chamber configuration from theoretical and experimental viewpoints. Accordingly, this paper assesses different configurations of the separation chambers through comprehensive CFD-based numerical and empirical investigations. Therefore, the main novelties and objectives of this study may be summarized as to: i) examine four innovative platforms for performance comparison purpose and eventually selecting the most favorable design; ii) compare separation and purification efficiency, energy consumption and pressure drop for the proposed concepts; iii) deep understand the airflow circumstances within the separation chambers; iv) study the effects of the suction condition and flow path on increasing and decreasing the losses and energy consumption of the systems; and v) investigate comprehensively CFD to examine precisely the separation and purification processes in agricultural equipments.

Material and methods

The proposed configurations were comprehensively analyzed and modeled to compare the corresponding performance of the separation chambers.

Separation chamber

The separation and purification chamber performance rely on the principle that the airflow transfers particles across a path which dimensions are larger than the dimensions of the other parts. Consequently, airspeed is decreased, and the particles are separated from the carrier air. Achieving a better separation performance relies on several specified conditions, which must be considered properly. In this regard, dimensions of the settling chamber, length (L) and height (H) of the chamber should be defined (Krupińska *et al.*, 2018). Accordingly, the separation chamber used in this work was constructed in accordance with the geometric variables proposed by Matin (1991). For this purpose, the pertinent dimensions were calculated using the following equations:

$$a = \sqrt{\frac{Q}{V_W}} \tag{1}$$

$$L = \frac{18\,\mu\,Q}{D^2 \rho_S\; g\; a} \tag{2}$$

where a = square dimension of chamber (m), L = length of chamber (m), Q = airflow (m^3/s), V_w = air velocity (m/s), μ = air dynamic viscosity (Ns/m^2), D = pods diameter (m), ρs = pods density (kg/m^3) and g = gravity acceleration (m/s^2). The corresponding chamber has a main suction duct (in the direction of the moving particles) and twofold side suction ducts (in the lower part of the chamber). In addition, in the compartment input field, an adjustable blade (0 to 90°) was placed to deviate the flow path. Moreover, a strong suction was provided implementing three high-pressure centrifugal fans. The main fan was mounted on the main suction duct, and two auxiliary side fans were used to enhance the suction performance. Meanwhile, the side fans were embedded inside the structure and the positioning of the fans was limited due to constraints in the geometry of the facility. To assess the suction circumstance and deviation of the streamline, four novel configurations of separation chamber were considered (Fig. 1) on the pre-experienced operation of the system: the chamber with main suction which supplies the required airflow (configuration I); the chamber with main suction and guide blade to deviate the flow path (configuration II); the chamber with main suction and twofold side suction – the side suctions can split the unswerving airstream (configuration III); and the chamber with main suction, flow deflective blade, and twofold side suctions, which is the combination of the above-mentioned configurations (configuration IV).

Separation efficiency and relative purification

Flow characteristics and required airflow were analyzed and compared in all the configurations. In addition, separation efficiency was calculated as:

$$\eta = \frac{S_s}{S_t} \tag{3}$$

where η = separation efficiency, S_s = sedimented pods and S_t = total feed pods to the chamber. To calculate the separation efficiency, 100 samples of pods were fed to the chamber (see Fig. 2a), after sedimentation of the pods, the numbers of separated pods counted and were inserted into Eq. (3). Furthermore, relative purification may be defined as:

$$RP = \frac{P_e}{P_t} \tag{4}$$

where RP = relative purification, P_e = eliminated hollow pods and P_t = total hollow pods. To calculate the relative purification, 100 samples of pods were selected, including 90 full pods and 10 hollow pods. The actual situation of harvested pods is presumed for the considered proportion, which has been illustrated in Fig. 2b.

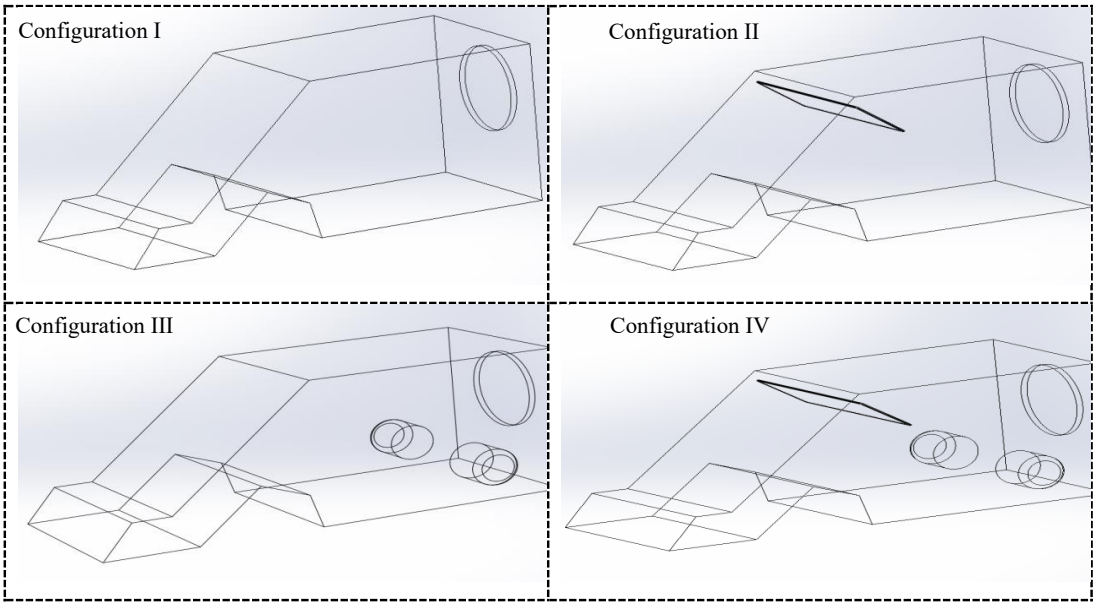

Figure 1. Proposed novel configurations for the separation chambers.

Experimental setup

An experimental investigation was carried out to compare the performance of the four proposed configurations of the separation chamber. Accordingly, the extracted velocity and pressure values were used to validate the numerical models. Fig. 3 shows the experimental setup consisting of the material transfer path, the main separation chamber, the main suction fan, the side fans, and the flow deflective blade. The fan was driven by an electrical motor (3.0 kW and 3000 rpm), and the rotational speed was adjusted by an inverter (LG-5A). Subsequently, the flow velocity and pressure were measured by a portable hot wire anemometer (MODEL 8465- TSI, resolution of 0.07 m/s, working range of 0.125–50 m/s) and a differential pressure meter (Model CPE310s- KIMO).

Meanwhile, four cross-sections were chosen for measuring the flow velocity and pressure at the position of *x*=5 cm, x=15 cm, *x*=25 cm, and *x*=35 cm as indicated in Fig. 4 with the numbers 1 to 4 along the x-axis. Furthermore, four points along the related height (y-axis) were investigated at the position of y=5 cm (points 1, 5, 9, and 13), y=15 cm (points 2, 6, 10, and 14), y=25 cm (points 3, 7, 11, and 15), and y=35 cm (points 4, 8, 12, and 16) from the top of the chamber to the bottom. For each point (overall 16 points), three measuring points were considered (along the z-axis) at the position of z=5, 15, and 25 (internal points). Moreover, the experimental results indicated a good agreement between z=5 and 25 cm since the axis-symmetric of these points concludes a similar outcome. Additionally, the measurements were conducted in advance of the main chamber for which three cross-sections were considered for the material transfer path, at the position of 1/4 (point 17), 2/4 (point 18), and 3/4 (point 19) of the transfer path length. The measurements were performed sufficiently away from the perforated walls to prevent the results from being affected because of the local effects of the embedded holes on the streamline.

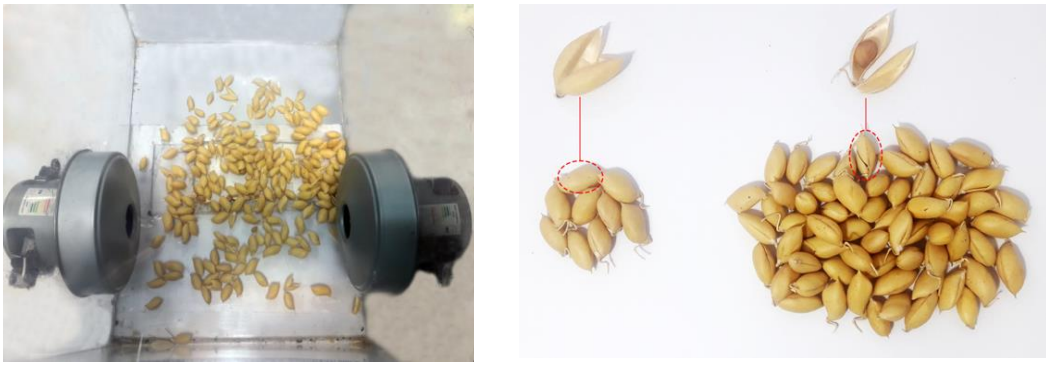

(a) (b)

Figure 2. Experimental assessment: (a) separated chickpea pods, (b) hollow and full chickpea pods.

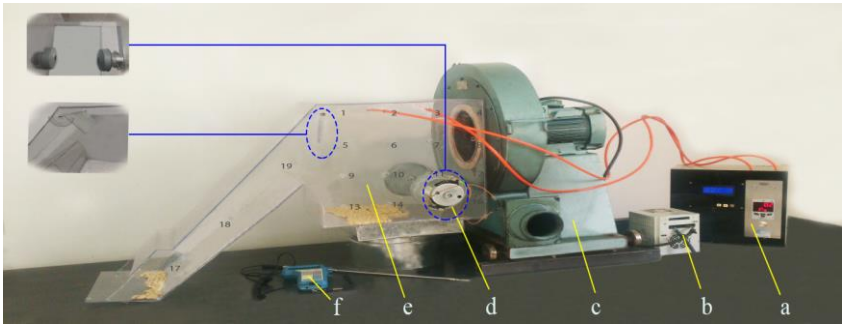

Figure 3. Proposed chamber and components of the experimental setup: (a) differential pressure meter, (b) inverter, (c) main fan, (d) side fans, (e) sedimentation chamber, and (f) anemometer.

The final values were considered to be the mean value of three replicated velocity and pressure values. The dimensions of the separation chamber and specifications of the system components are listed in Table 1.

Grid division

Fig. 5 depicts the tetrahedral mesh generated for the chamber for simulation purposes. Grid independence test was also scrutinized to ensure grid independency of the outcomes and also to ascertain the medium-sized grid for fast and efficient convergence. In order to attain accurate results, finer grids were generated for the deflective blade and side fans.

CFD modeling

In order to assess the internal airflow pattern, the proposed concepts of the separation chamber were analyzed by CFD simulation. Ansys Fluent package was used to solve the correlated equations for the whole proposed concepts. The coupled solver is recommended for transonic and supersonic flows. On the other hand, the segregated solver is much faster for low-speed flows and is more appropriate for incompressible flows, showing good performance for simulating subsonic compressible flows; so, it was used in this study (Ansys Fluent, 2013). A flowchart describing the simulation procedure in Ansys Fluent is showed in Fig. S1 [suppl.].

Governing equations and turbulence model

For the flow simulation purpose, continuity and momentum equations were solved in three dimensions for the superficial air velocities and pressure distribution.

Continuity equation:

$$\frac{\partial \rho}{\partial t} = \frac{\partial}{\partial x_i}\left(\rho u_j\right) \quad (5)$$

Momentum equation:

$$\frac{\partial}{\partial t}\left(\rho u_i\right) + \frac{\partial}{\partial x_j}\left(\rho u_i u_j\right) = \frac{\partial}{\partial x_i}\left[-p\delta_{ij} + \mu\left(\frac{\partial u_i}{\partial x_j} + \frac{\partial u_j}{\partial x_i}\right)\right] + \rho g_i \quad (6)$$

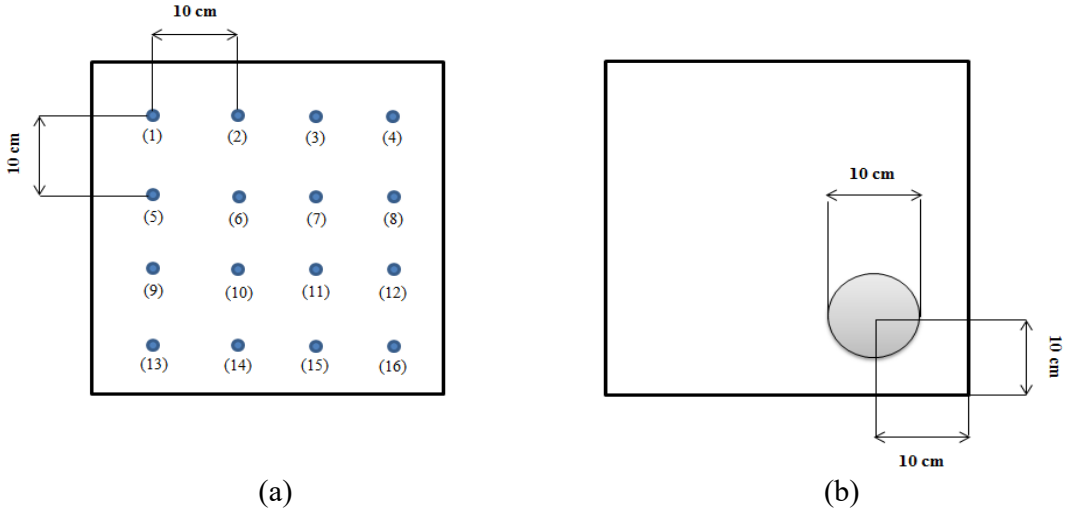

Figure 4. A schematic view of points (a) and side fans position (b).

Table 1. Specifications of the separation and purification system.

Variables	Value
Main chamber cross- section (width × height) (m)	0.3 × 0.3
Main chamber length (m)	0.4
Flow deviation blade (width × height) (m)	0.3 × 0.1
Diameter of main suction duct (m)	0.2
Diameter of side suction ducts (m)	0.1
Maximum air flow of main fan (m^3/hr)	2500
Maximum air flow of side fans (m^3/hr)	192

where ρ = density (kg/m^3), t = time (s), u_i and u_j are the average superficial velocity component in i and j directions, respectively (m/s), p = pressure (Pa), g_i = acceleration due to gravity (m/s^2), μ = viscosity (Pa·s) and i, j = 1, 2, 3 (x, y, z).

The inlet Reynolds number of the flow was found higher than 5000 in all proposed separation chamber configurations. Accordingly, the $k-\varepsilon$ model, one of the most common and widely used turbulence models, was used. The $k-\varepsilon$ model is supported by two equations:

— Turbulent kinetic energy (k) equation:

$$\frac{\partial(\rho k)}{\partial t}+\frac{\partial(\rho k u_i)}{\partial t}=\frac{\partial}{\partial x_j}\left[\frac{\mu_t}{\sigma_k}\frac{\partial k}{dx_j}\right]+2\mu_t E_{ij}E_{ij}-\rho\varepsilon \quad (7)$$

— Dissipation (ε) equation:

$$\frac{\partial(\rho\varepsilon)}{\partial t}+\frac{\partial(\rho\varepsilon u_i)}{\partial x_i}=\frac{\partial}{\partial x_j}\left[\frac{\mu_t}{\sigma_\varepsilon}\frac{\partial\varepsilon}{\partial x_j}\right]+C_{1\varepsilon}\frac{\varepsilon}{k}2\mu_t E_{ij}E_{ij}-C_{2\varepsilon}\rho\frac{\varepsilon^2}{k} \quad (8)$$

$$\mu_t=\rho C_\mu\frac{k^2}{\varepsilon} \quad (9)$$

where u_i = velocity component in corresponding direction (m/s), C_μ, $C_{1\varepsilon}$, $C_{2\varepsilon}$, σ_k and σ_ε = constants, E_{ij} = component of rate of deformation (1/s), σ = turbulent based on Prandtl number, and μ_t = mean turbulent viscosity. For a better convergence, the residuals have been stabilized at 10^{-4} for the equations of continuity and momentum. The values of these constants have been arrived by numerous iterations of data fitting for a wide range of turbulent flows as (Ansys Fluent, 2013): C_μ = 0.09; σ_k = 1.00; σ_ε =1.30; $C_{1\varepsilon}$ =1.44; $C_{2\varepsilon}$ =1.92.

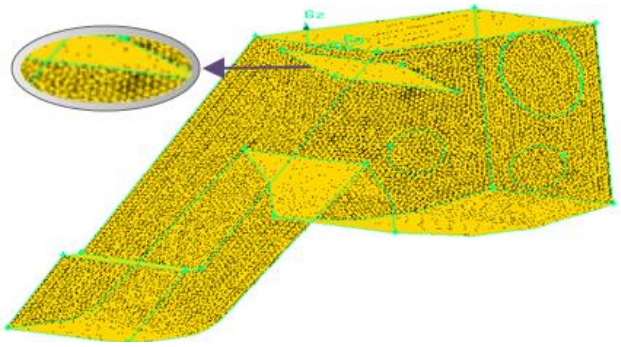

Figure 5. Generated tetrahedral grid for the chamber in Gambit software.

Discretization scheme

The entire separation chamber was considered as a control volume to perform a 3D numerical assessment for the proposed configurations. To ensure the grid independency results, three grid domains were tested in our preliminary computation *i.e.*, fine (541,286 cells), medium (314,520 cells), and coarse (185,126 cells). The difference in the results was less than 5% for the pressure results. In this regard, computational domain considered having 314,520 cells (medium size grid) for the generated grid. Meanwhile, the entire computational domain was generated using tetrahedral volume cells and the discretization was conducted based on the most satisfactory grid resolution required for the RANS simulation. Noteworthy, to have a satisfactory accuracy, a fine grid was generated for the zones near the employed fans and the separation part. On the other hand, for the other parts of the domain, medium size grid was generated accordingly.

Boundary conditions

Getting accurate results from the CFD model strongly depends on the correct definition of the boundary conditions. Accordingly, three different boundary conditions were used in this work: inlet velocity, outlet pressure, and the walls. For all simulations, the outlet pressure was fixed as atmospheric pressure for the outlet boundary. No-slip conditions were assumed for the corresponding walls. In order to have a reliable turbulence simulation near the walls, finer elements were used in the boundary layer (Rong *et al.*, 2011).

Validation

We used velocity and pressure data to validate the experimental data with CFD simulations. Moreover, the pods behavior was better observed by the High Speed Photography (HSPh) technique in all configurations. In order to eliminate the effect of pod sizes on motion trajectory, tracking experiments were repeated three times for each configuration. To validate results, Lan *et al.* (1999) and Panning *et al.* (2000) used optoelectronic sensors, and Karayel *et al.* (2006) and Zhan *et al.* (2010) applied smoke tests and high-speed camera system sensors.

Results

The results of the modeling and also the corresponding outcomes of the empirical investigations are presented for the proposed separation chambers. For this purpose, some critical variables are considered to assess the performance of the proposed configurations.

System performance

Separation efficiency is assumed as first chosen critical factor, and the effect of this parameter was scrutinized accordingly. The results of the experimental tests indicated that employing a deflective as the second concept and the side fans as the third proposed concept increased the separation efficiency by 6% and 10%, respectively. Meanwhile, implementing both deflective blade and side fans can potentially increase the efficiency by 15%. It should be noted that the increment of the efficiency as a result of employing side fans was 4% higher in comparison with using a solely deflective blade. The corresponding results are listed in Table 2.

Relative purification as one of the foremost effective parameters is also assessed for the proposed concepts. Accordingly, the outcomes of the correlative empirical investigations are presented in Table 2. Considering the configuration I, due to the low density of hollow pods, a significant number of pods moved in a direct pathway when entering the chamber, thereafter were debarked from sediment pods. Considering configuration II, collision of the hollow pod with the guide blade resulted in falling some of the hollow pods into the separation chamber. On the other hand, in configuration III with side fans, the pathway of the pods and the carrier fluid deviate downward, which may sediment some hollow pods.

Comparing the employ of a guide blade and side fans revealed that the guide had an unfavorable effect higher than 30%.

Furthermore, the required airflow rate was also another critical variable considered. When separation efficiency reached a peak, the required airflow rate for the 2nd, 3rd, and 4th proposed configurations would fall by 6.67%, 29.05% and 35.71%, respectively as compared to the conventional chamber (configuration I). Accordingly, designing the corresponding parameters properly, *i.e.*, deflective blade, and the side fans, can enhance the separation efficiency. In addition to the aforementioned results, a significant reduction is expected for the required airflow for the chamber, which is roughly equivalent to the reduction of the energy use.

It is worth bearing in mind that, among the investigated parameters, the descent effect of the side fans was more significant on the airflow reduction. The positive influence of the side fans was 22.38 % higher than the guide blade on the required airflow.

Flow characteristics

Velocity magnitude

Fig. S2 [suppl.] shows that the velocity magnitude of the simulation results was in good agreement with the experimental data, considering all proposed configurations. Good agreement was achieved in three (5, 15, and 25 cm) internal points, namely 1st, 2nd, 3rd, respectively. According to the symmetric geometry of the chamber, the final results are only presented for 5 and 15 cm internal points (1st and 2nd). Velocity variations in numerical results were a little bit higher than experimental data.

Fig. 6a shows that, in preliminary points of 1st internal point, the change in the velocity magnitude was significant, which was mainly due to the deflective blade and the side suction fans. The outcomes revealed that employing the guide blade and the side fans can potentially raise the velocity magnitude at points 5 to 8 while it was not effective on points 9 to 14. As can be seen in Table 2, the required airflow rate was not identical for concluding the maximum efficiency in different configurations. On the other hand, since point 17 is located in the cross-section area, the velocity difference in the chambers would be significant. A similar trend was observed for the numerical results (Fig. 6b). Moreover, the variations of velocity for 2nd internal points are presented in Figs. 6c and 6d. In comparison to the 1st internal points, at 2nd ones the experimental results of configuration II were approximately closer to configurations III and IV. This can be justified because the positions of the 2nd points are not close to the side

Table 2. Separation efficiency, relative purification, and required airflow in various chamber configurations.

Different designs of chamber	Separation efficiency (%)	Relative purification (%)	Air flow(m^3/h)
Configuration I	80	90	847.8
Configuration II	86	30	791.2
Configuration III	90	60	601.5
Configuration IV	95	50	545.0

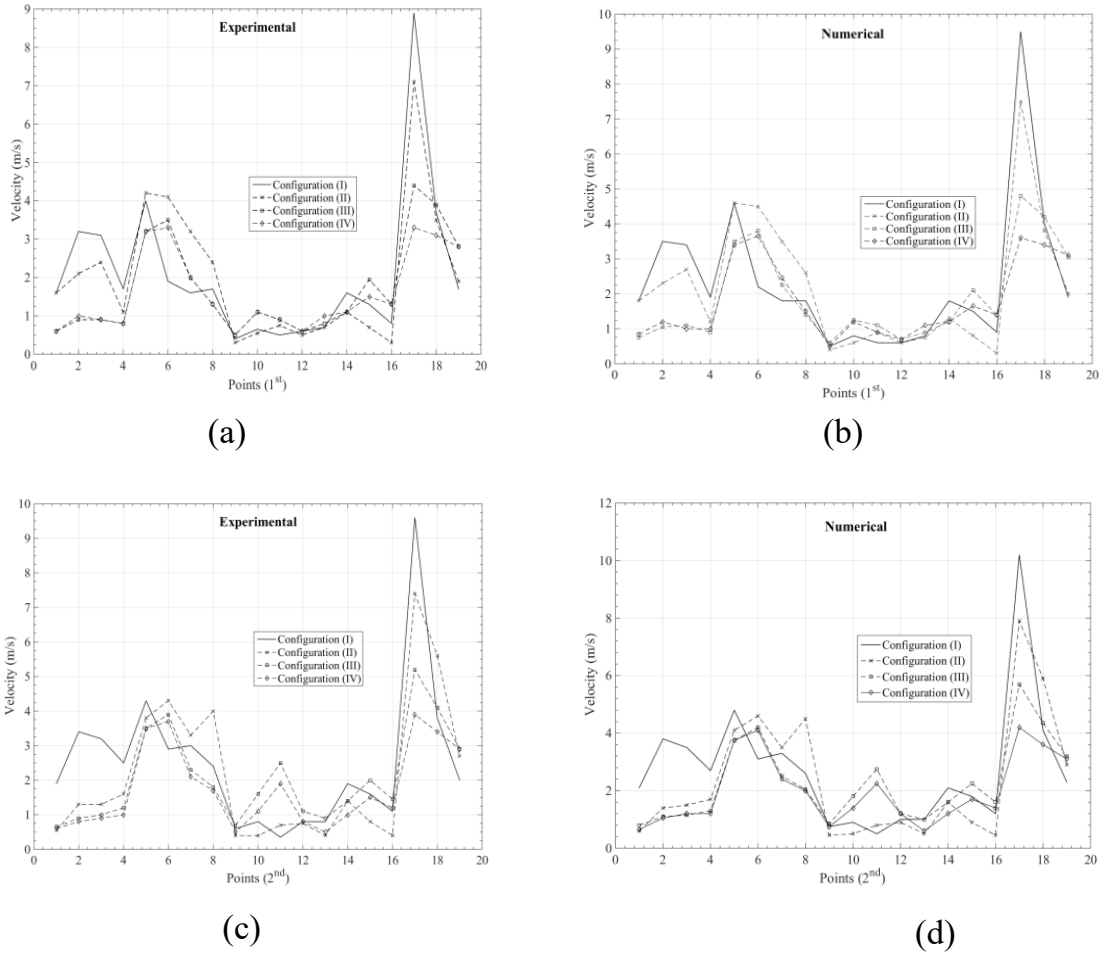

Figure 6. Experimental results of velocity magnitude for various points in the proposed configurations (a: 1st internal point; c: 2nd internal point). Numerical outcomes of velocity magnitude for various points in the proposed configurations (b: 1st internal point; d: 2nd internal point).

fans (in 1st points, main suction is amplified by side fans). The same trend was observed for the numerical results.

Pressure field

Fig. S3 [suppl.] illustrates the pressure drop value in the proposed configurations. Meantime, the correlative comparison between the experimental and numerical data showed a good agreement for the proposed configurations. That is correct in both internal points (1st and 2nd). Noteworthy, in all the designed configurations, the pressure variation showed a relatively consistent trend, while the only disorder was seen for 4, 8, 12 and 16 points, because they are close to the main suction.

Considering 1st and 2nd internal points, as shown in Figs. 7a and 7c, the most critical issue about experimental results regarding pressure drop is the significant difference between the various points and conditions. For example, at the primary internal points, at point 1, configuration I shows the highest pressure drop, while the minimum measured pressure drop was found with configuration III. Accordingly, the impact of the side fans on the pressure drop was significant. Pressure drop in configuration I was 54% higher than in configuration III. However, a change in the aforementioned trend was observed at points 2 and 3, with a slight difference between the proposed configurations. The mentioned differences were mainly related to the geometrical location, which may influence the compressibility of the intake flow resulted from the guide blade and the side suction fans. Overall, the lowest pressure drop difference was accounted at point 7, which showed the value of 2.9% for the assumed configurations. At this point, the effect of the main suction was dominant due to the effects of the deviation blade and the side fans. It is worth mentioning that the related trend between 1st and 2nd internal points was similar. However, a critical problem caused at the following internal points (Fig. 7c) was that the highest pressure drop occurred in configuration I. The numerical results obtained for the calculated pressure drop are presented in Figs. 7b and 7d.

Velocity and pressure visualizations

To have a deep understanding of pressure and velocity distributions and the correlative profiles, dynamic pressure contours and velocity magnitude vectors are presented in Fig. 8. The CFD modeling results indicated that the highest and lowest values of dynamic pressure were 124 Pa and 16.3 Pa, respectively, associated with configurations I and IV, respectively. The highest velocity (15.6 m/s) was obtained with configuration I, while the lowest (5.85 m/s) with configuration IV.

It was found that the employed blade and the side fans had a positive effect on separation efficiency. As shown in Fig. 8b, using the guide blade may change the concentration of dynamic pressure contours from the zone (1) to the zone (2). Accordingly, these changes caused a lower pod entrance to the chamber outlet and hence increased the separation efficiency (Figs. 9a and 9b). Implementing the side fans can significantly transfer the concentration from the zone (1) to zone (2) and completely to zone (3), indicating that the side fans have more influence on separation efficiency (Fig. 9). An important result is that using a deflective blade along with the side fans can change the focus to the zone (3), which results in 95% separation efficiency. Figs. 9c and 9d show the location of the pods for which the HSPh technique was used.

In configuration I, the velocity magnitude is substantial in zone (1), hollow pods across their pathway can leave the chamber (are suctioned by the main fan), and so the purification would be accomplished completely. As shown in Fig. 8b, considering configuration II, the dynamic pressure and velocity were concentrated in zone (2) which is mainly because of applying the deflective blade. Accordingly hollow pods, after reaching the blade, move downward of the chamber. Consequently, a great number of hollow pods firstly enter the zone (3), and segregate thereafter. On the other hand, some of them are mounted to the main flow located in the zone (2) and leave the chamber outlet (Fig. 9b). In configuration III, the hollow pods enter the chamber directly with no deviation in the pathway (Fig. 9c). On the other hand, in configuration III, the distribution of the dynamic pressure and velocity magnitude was weak due to a wide range of the flow *i.e.*, extensive dispersion of the stream because of downward suction of the side fans. Consequently, purification was firstly increased in comparison with

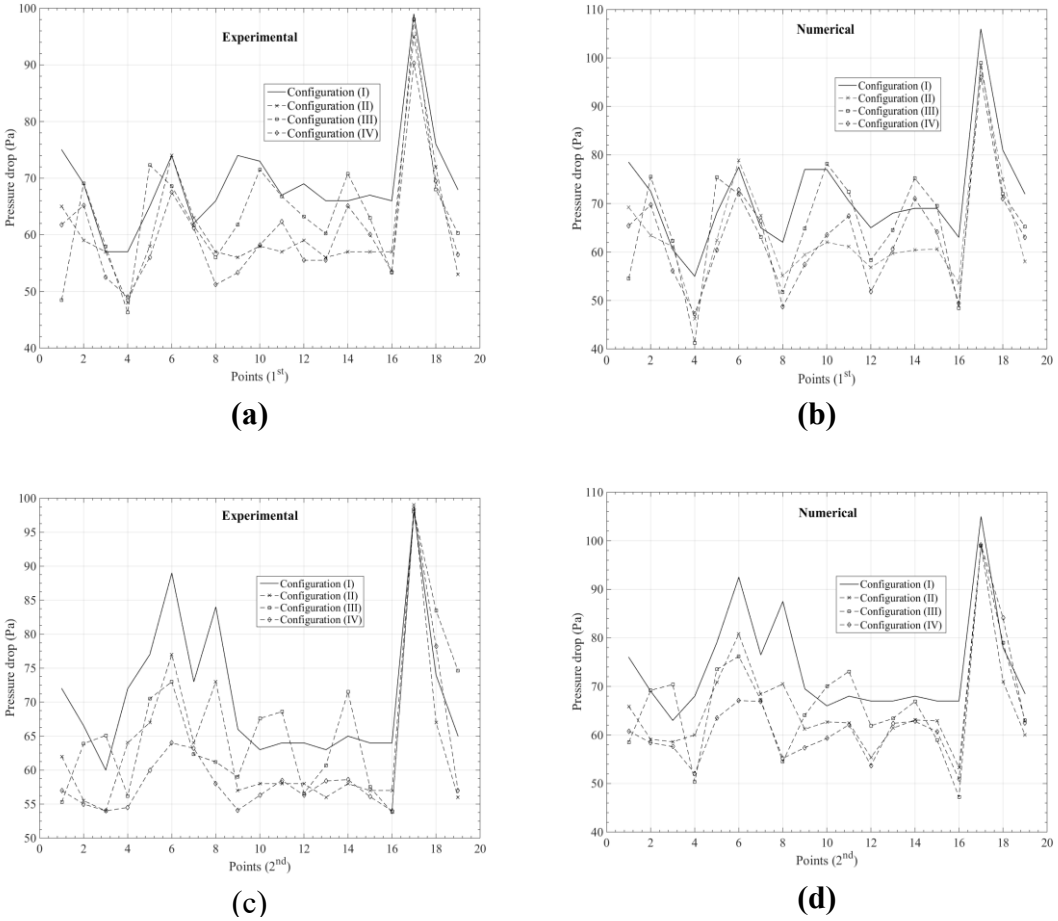

Figure 7. Experimental results of the pressure drops for various points in four configurations (a: 1st internal point; c: 2nd internal point). Numerical results of pressure drop for various points in four configurations (b: 1st internal point; d: 2nd internal point)

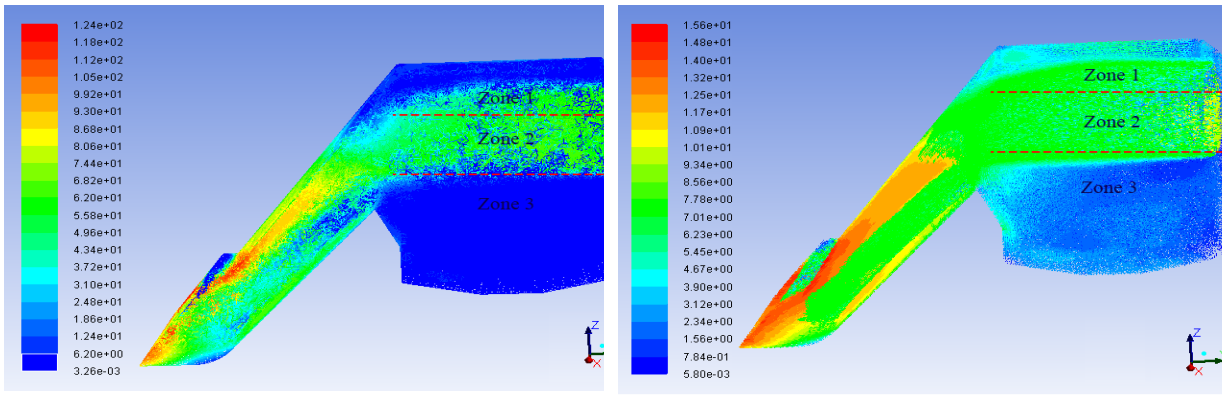

(a)

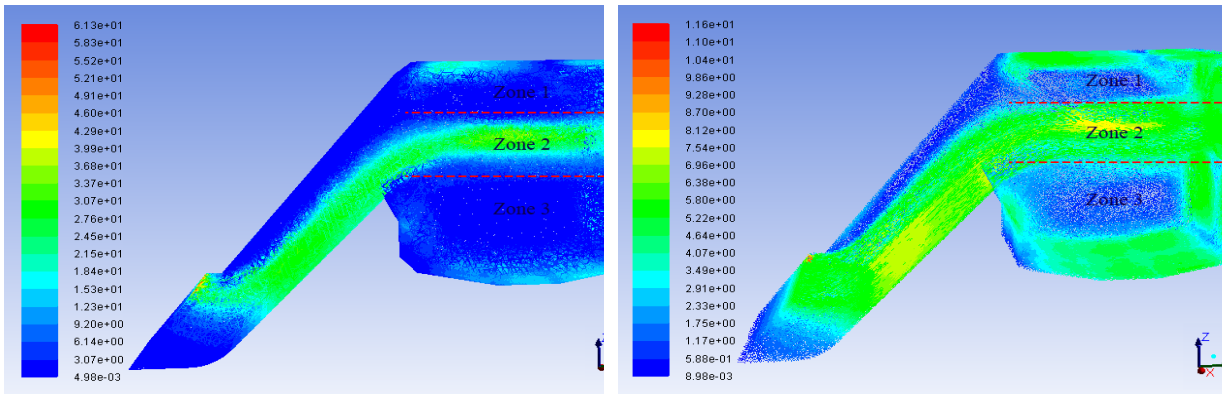

(b)

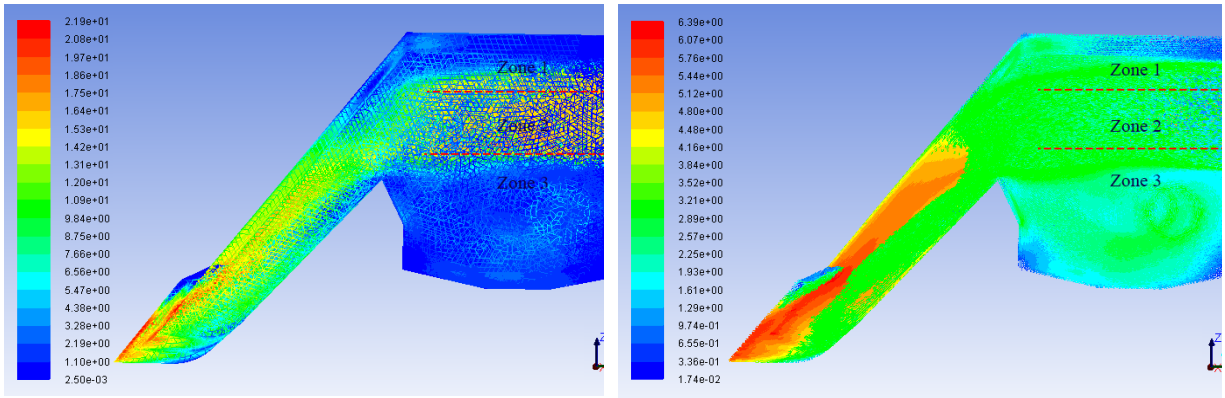

(c)

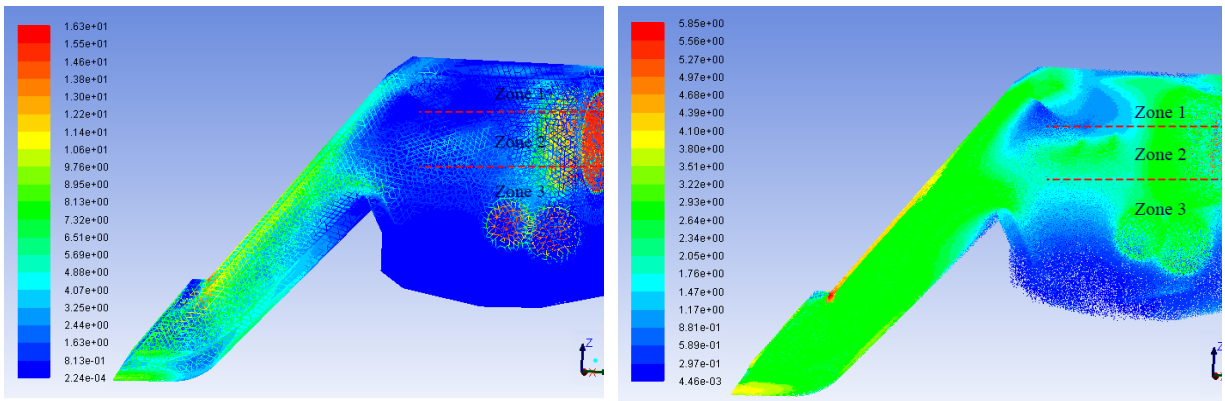

(d)

Figure 8. Configuration I (a), II (b), III (c) and IV (d): dynamic pressure contour, Pa (left) and velocity magnitude vector, m/s (right)

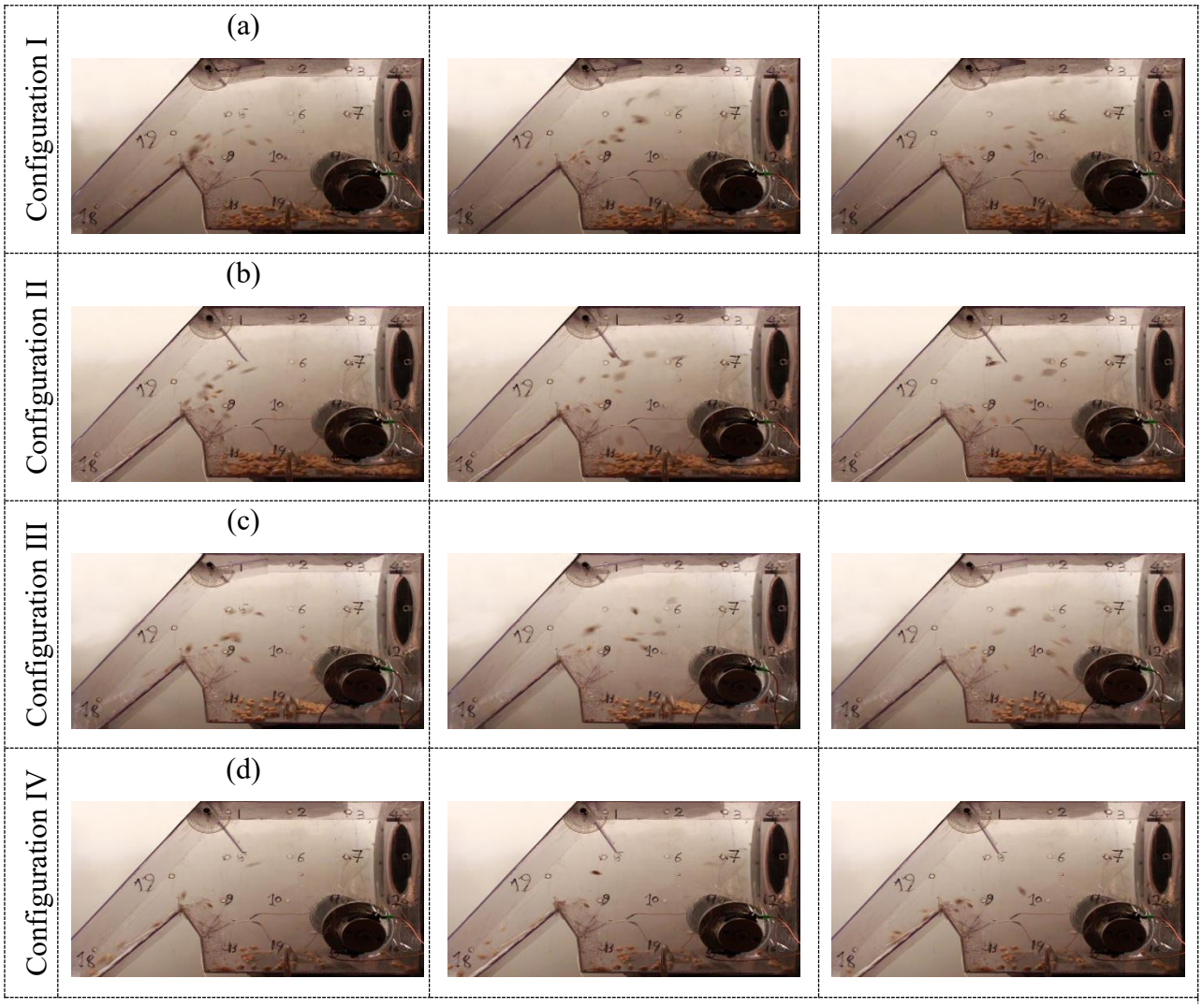

Figure 9. High speed photography (HSPh) for different proposed configurations

the configuration II because the pods entered the chamber straightly. Secondly, purification was decreased in comparison with the configuration I since the dynamic pressure and velocity magnitude was not considerable inside the chamber itself. As shown in Fig. 8d, the movement of the hollow pods in the configuration IV was similar to the configuration II. The corresponding similarity can be explained because some segregated hollow pods are mounted to the side fans flow beside impacted by the main suction and would leave the chamber (Fig. 9d). The aforementioned phenomenon occurred mainly for using the side fans and extensive velocity coverage. Consequently, the relative purification performance may be improved in comparison with configuration II.

Discussion

A comprehensive assessment of flow behavior was carried out for four innovative configurations of the separation and purification chambers. Along with CFD, experimental tests were conducted to calibrate separation efficiency, relative purification and required airflow. Furthermore, the effects of the deflective blade, and the side fans were investigated for the proposed configurations. Both deflective blade and side fans increased the separation efficiency and decreased the required airflow (required energy). The deflective blade and side fans would decrease purification performance, while the blade may conclude some unfavorable repercussions. Implementing configuration IV would be a better choice since it leads to the highest separation efficiency among the proposed concepts. From the viewpoint of relative purification, the first proposed system has the highest corresponding value (90%) and is strongly recommended to be employed. The lowest value for the required airflow or energy consumption is associated with configuration IV. For the case of dynamic pressure, the configuration I performed unfavorable with the value of 124 Pa, whiles the performance of configuration IV was favorable (16.3 Pa). To sum up,

it can be concluded that configuration IV is the optimum proposed design because of the minimum pressure drop, required airflow (energy usage), and maximum resulted in separation efficiency. In conclusion, a combined novel system consisting of configuration I and IV in which configuration I located at the first part and accordingly correlated segregated pods would enter the second part where the configuration IV was employed. The proposed concept (as the optimal configuration) may bring some substantial benefits *i.e.*, achieving the highest separation efficiency and relative purification at the same time concluding the lowest required airflow. Eventually, some suggestions for future studies are: implementing the proposed combined separation and purification chamber for industrial purposes on different scales; investigating the economic aspects of the proposed combined separation chamber from different perspectives; and optimizing the proposed combined separation chamber considering total associated cost with the system and separation/purification efficiency.

References

Ansys Fluent, 2013. Ansys Fluent Theory Guide. Release 18.2 15317, pp: 373-464.

Burtally N, King PJ, Swift MR, 2002. Spontaneous air-driven separation in vertically vibrated fine granular mixtures. Science 295: 1877-1879. https://doi.org/10.1126/science.1066850

Chen L, Jin X, Yang L, Du X, Yang Y, 2017. Particle transport characteristics in indoor environment with an air cleaner: The effect of nonuniform particle distributions. Build Simul 10: 123-133. https://doi.org/10.1007/s12273-016-0310-7

Chen L, Wu Y, Dong H, Meng M, Li C, Yan Y, Chen J, 2018. An overview on membrane strategies for rare earths extraction and separation. Sep Purif Technol 197: 70-85. https://doi.org/10.1016/j.seppur.2017.12.053

Chimakurthi SK , Reuss S, Tooley M, Scampoli S, 2018. ANSYS Workbench System Coupling: A state-of-the-art computational framework for analyzing multiphysics problems. Eng Comput 34: 385-411. https://doi.org/10.1007/s00366-017-0548-4

Devarrewaere W, Heimbach U, Foqué D, Nicolai B, Nuyttens D, Verboven P, 2016. Wind tunnel and CFD study of dust dispersion from pesticide-treated maize seed. Comput Electron Agr 128: 27-33. https://doi.org/10.1016/j.compag.2016.08.007

Elsayed Khairy K, Lacor C, 2010. Optimization of the cyclone separator geometry for minimum pressure drop using mathematical models and CFD simulations. Chem Eng Sci 65: 6048-6058. https://doi.org/10.1016/j.ces.2010.08.042

Emami S, Tabil L G, Tyler RT, Crerar WJ, 2007. Starch-protein separation from chickpea flour using a hydrocyclone. J Food Eng 82: 460-465. https://doi.org/10.1016/j.jfoodeng.2007.03.002

Gebrehiwot MG, De Baerdemaeker J, Baelmans M, 2010. Effect of a cross-flow opening on the performance of a centrifugal fan in a combine harvester: Computational and experimental study. Biosyst Eng 105: 247-256. https://doi.org/10.1016/j.biosystemseng.2009.11.003

Gharakhani H, Alimardani R, Jafari A, 2017. Design a new cutter-bar mechanism with flexible blades and its evaluation on harvesting of lentil. Eng. Agric. Environ. Food 10, 198-207. https://doi.org/10.1016/j.eaef.2017.03.001

Golpira H, Tavakoli T, Baerdemaeker JD, 2013. Design and development of a chickpea stripper harvester. Span J Agric Res 11: 929-934. https://doi.org/10.5424/sjar/2013114-3393

Goula AM, Karapantsios TD, Achilias DS, Adamopoulos KG, 2008. Water sorption isotherms and glass transition temperature of spray dried tomato pulp. J Food Eng 85: 73-83. https://doi.org/10.1016/j.jfoodeng.2007.07.015

Ha G, Kim E, Kim Y, Lee J, Ahn Y, Kim D, 2011. A study on the optimal design of a cyclone system for vacuum cleaner with the consideration of house dust. J Mech Sci Technol 25: 689-694. https://doi.org/10.1007/s12206-011-0122-8

Huang AN, Kuo HP, 2017. CFD simulation of particle segregation in a rotating drum. Part I: Eulerian solid phase kinetic viscosity. Adv Powder Technol 28: 2094-2101. https://doi.org/10.1016/j.apt.2017.05.016

Huang AN, Kuo HP, 2018. CFD simulation of particle segregation in a rotating drum. Part II: Effects of specularity coefficient. Adv Powder Technol 29 (12): 3368-3374. https://doi.org/10.1016/j.apt.2018.09.019

Karayel D, Wiesehoff M, Özmerzi A, Müller J, 2006. Laboratory measurement of seed drill seed spacing and velocity of fall of seeds using high-speed camera system. Comput Electron Agric 50: 89-96. https://doi.org/10.1016/j.compag.2005.05.005

Kozołub P, Klimanek A, Białecki RA, Adamczyk WP, 2017. Numerical simulation of a dense solid particle flow inside a cyclone separator using the hybrid Euler-Lagrange approach. Particuology 31: 170-180. https://doi.org/10.1016/j.partic.2016.09.003

Krupińska A, Ochowiak M, Włodarczak S, 2018. Selected aspects of dust removal from gas stream for chamber separators. In: Practical aspects of chemical engineering; Mitkowski PT *et al.*, Elsevier, pp: 217-229. https://doi.org/10.1007/978-3-319-73978-6_15

Lan Y, Kocher MF, Smith JA, 1999. Opto-electronic sensor system for laboratory measurement of planter seed spacing with small seeds. J Agr Eng Res 72: 119-127. https://doi.org/10.1006/jaer.1998.0353

Matin AH, 1991. A guide to design and calculation for industrial hygienists. University of Tehran Press, 34805.

Miller SA, 2014. Mechanical separation techniques. AccessScience, McGraw-Hill Education

Möbius ME, Lauderdale BE Nagel SR, Jaeger HM, 2001. Size separation of granular particles. Nature 414: 270. https://doi.org/10.1038/35104697

Molerus O, Glückler M, 1996. Development of a cyclone separator with new design. Powder Technol 86: 37-40. https://doi.org/10.1016/0032-5910(95)03035-2

Motlagh AM, Rostampour V, Mardani K, 2018. Design, fabrication and evaluation of a short-legged chickpea harvest machine. Iran Biosyst Eng 49: 83-94.

Narasimha M, Brennan MS, Holtham PN, 2012. CFD modeling of hydrocyclones: Prediction of particle size segregation. Miner Eng 39: 173-183. https://doi.org/10.1016/j.mineng.2012.05.010

Olatunde GA, Atungulu GG, Smith DL, 2017. One-pass drying of rough rice with an industrial 915 MHz microwave dryer: Quality and energy use consideration. Biosyst Eng 155: 33-43. https://doi.org/10.1016/j.biosystemseng.2016.12.001

Panasiewicz M, Sobczak P, Mazur J, Zawiślak K, Andrejko D, 2012. The technique and analysis of the process of separation and cleaning grain materials. J Food Eng 109: 603-608. https://doi.org/10.1016/j.jfoodeng.2011.10.010

Panning JW, Kocher MF, Smith JA, Kachman SD, 2000. Laboratory and fıeld testıng of seed spacıng unıformıty for sugarbeet planters. Appl Eng Agr 16: 7-13. https://doi.org/10.13031/2013.4985

Rezvanivand Fanayi A, Nikbakht AM, 2015. A CFD study of the effects of feed diameter on the pressure drop in acyclone separator. Int J Food Eng 11: 71-77. https://doi.org/10.1515/ijfe-2014-0125

Rezvanivand-Fanaei A, Hasanpour A, Nikbakht AM, 2020. Study of the vapor thermo-compressor to reduce energy consumption in the sugar production line using computational fluid dynamics. J Agr Machin 10: 241-253.

Rezvanivand-Fanaei, Nikbakht AM, A, Hasanpour A, 2021. A Computational-Experimental Investigation of Thermal Vapor Compressor as an Energy Saving Tool for the Crystallization of Sugar in a Sugar Processing Plant. J Food Process Eng.

Rong L, Elhadidi B, Khalifa HE, Nielsen PV, Zhang G, 2011. Validation of CFD simulation for ammonia emissions from an aqueous solution. Comput Electron Agric 75: 261-271. https://doi.org/10.1016/j.compag.2010.12.002

Schaldach G, Berndt H, Sharp BL, 2003. An application of computational fluid dynamics (CFD) to the characterisation and optimisation of a cyclonic spray chamber for ICP-AES. J Anal At Spectrom 18: 742-750. https://doi.org/10.1039/b302052e

Scotto di Perta E, Agizza MA, Sorrentino G, Boccia L, Pindozzi S, 2016. Study of aerodynamic performances of different wind tunnel configurations and air inlet velocities, using computational fluid dynamics (CFD). Comput Electron Agric 125: 137-148. https://doi.org/10.1016/j.compag.2016.05.007

Tian J, Ni L, Song T, Olson J, Zhao J, 2018. An overview of operating parameters and conditions in hydrocyclones for enhanced separations. Sep Purif Technol 206: 268-285. https://doi.org/10.1016/j.seppur.2018.06.015

Wei J, Zhang H, Wang Y, Wen Z, Yao B, Dong J, 2017. The gas-solid flow characteristics of cyclones. Powder Technol 308: 178-192. https://doi.org/10.1016/j.powtec.2016.11.044

Wu X, Wang X, Zhou Y, 2018. Experimental study and numerical simulation of the characteristics of a percussive gas-solid separator. Particuology 36: 96-105. https://doi.org/10.1016/j.partic.2017.04.007

Zhan Z, Yaoming L, Jin C, Lizhang X, 2010. Numerical analysis and laboratory testing of seed spacing uniformity performance for vacuum-cylinder precision seeder. Biosyst Eng 106: 344-351. https://doi.org/10.1016/j.biosystemseng.2010.02.012

Zhao Z, Li Y, Chen J, Xu J, 2011. Grain separation loss monitoring system in combine harvester. Comput Electron Agric 76: 183-188. https://doi.org/10.1016/j.compag.2011.01.016